Acta Crystallographica Section F
Structural Biology and Crystallization Communications
ISSN 1744-3091

Purification, crystallization and preliminary crystallographic analysis of mouse *myo*-inositol oxygenase

Peter M. Brown,[a,b]* Tom T. Caradoc-Davies,[a,b] James M. Dickson,[a,b] Garth J. S. Cooper,[a,b] Kerry M. Loomes[a,b] and Edward N. Baker[a,b]

[a]Centre for Molecular Biodiscovery, University of Auckland, Private Bag 92019, Auckland, New Zealand, and [b]School of Biological Sciences, University of Auckland, Private Bag 92019, Auckland, New Zealand

Correspondence e-mail: pbro100@ec.auckland.ac.nz

Received 22 June 2006
Accepted 20 July 2006

Myo-inositol oxygenase (MIOX) catalyzes the novel oxidative cleavage of *myo*-inositol (MI) and its epimer D-*chiro* inositol (DCI) to D-glucuronate. MIOX utilizes an Fe^{II}/Fe^{III} binuclear iron centre for the dioxygen-dependent cleavage of the C1—C6 bond in MI. Despite its key role in inositol metabolism, the structural basis of its unique four-electron oxidation mechanism and its substrate specificity remain unknown. In order to answer these questions and to facilitate the use of this key enzyme for the development of new therapeutic strategies for diabetes, the mouse enzyme has been cloned, expressed in *Escherichia coli*, purified and crystallized from 4.4 *M* sodium formate. The crystals belong to space group $P2_12_12_1$, with unit-cell parameters a = 44.87, b = 77.26, c = 84.84 Å, and diffract to 2.8 Å resolution.

1. Introduction

Diabetes mellitus (DM) is a major global health concern, the prevalence of which has risen dramatically in recent decades owing to changes in diet and lifestyle. Importantly, the morbidity and mortality associated with DM is largely attributed to its complications, including coronary and cerebrovascular disorders, peripheral arterial disease, nephropathy and retinopathy (Khan *et al.*, 2006). These complications result from sustained hyperglycaemia and are believed to develop through a number of pathways, including non-enzymatic glycation processes, increased aldose reductase activity and alteration of the protein kinase C pathway (Brownlee, 2000).

Myo-inositol oxygenase (MIOX), consisting of 285 residues (33.2 kDa), is an enzyme implicated in diabetic complications owing to its ability to catalyze an oxidative cleavage of the inositol compounds *myo*-inositol (MI) and its epimer D-*chiro* inositol (DCI) between C-1 and C-6 of the inositol ring to form glucuronic acid (Fig. 1). This reaction occurs predominantly in the kidney, where MIOX is found almost exclusively (Arner *et al.*, 2006), and is the only known route of inositol catabolism. As this oxidative cleavage is the first step in the glucuronate-xylulose pathway, MIOX potentially plays an important role in the regulation of endogenous inositol levels, which are involved in many aspects of cellular regulation (Arner *et al.*, 2001). Altered inositol metabolism is associated with diabetes and insulin resistance, while administration of DCI has been shown to lower blood glucose and improve insulin action (Ortmeyer *et al.*, 1993). As MIOX expression and activity is increased in diabetes (Nayak *et al.*, 2005), its inhibition under these circumstances may therefore represent a promising strategy for raising depleted inositol levels.

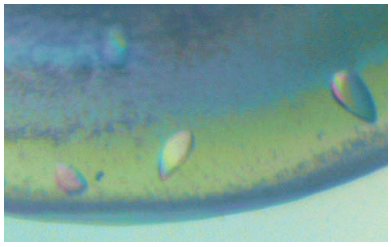

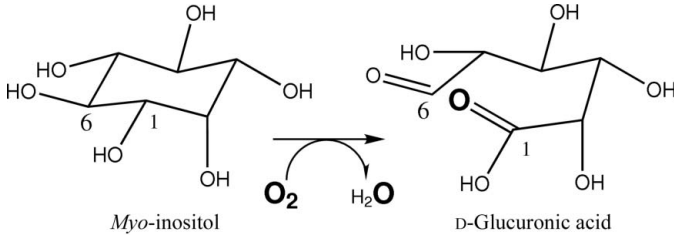

Figure 1
The first step of the glucuronate-xylulose pathway catalyzed by *myo*-inositol oxygenase (MIOX).

MIOX has previously been described as a renal-specific oxidoreductase with an NADPH-binding sequence motif (MAKS), as seen in the mouse MIOX sequence (Yang *et al.*, 2000). However, as other mammalian MIOX sequences lack this motif, this classification has been under debate. More recently, MIOX has been characterized spectroscopically as a non-haem di-iron oxygenase with a mechanism that utilizes an Fe^{II}/Fe^{III} binuclear iron centre for catalysis (Xing *et al.*, 2006).

MIOX is highly conserved across all mammals, plants and microorganisms, yet shows no homology with other proteins based on sequence similarity. Pairwise sequence alignments of mammalian MIOX show ∼90% amino-acid sequence identity, strongly suggesting a conserved and essential function (Arner *et al.*, 2006). Solution of the crystal structure of MIOX will allow discovery of its polypeptide fold and active-site architecture, which are currently unknown, and potentially yield new insights into the reaction mechanism. Here, we describe the cloning, expression, purification and crystallization of mouse MIOX, together with preliminary crystallographic data from these crystals.

2. Methods and results

2.1. Cloning, expression and purification

The DNA fragment encoding mouse MIOX (accession No. AY738257) was amplified by PCR from *Mus musculus* genomic DNA using the primers miox-N-term-fwd (5′-ATACCATGGGAATGAAGGTCGATGTGG-3′) and miox-C-term-rev (5′-TATGAA TCCTCACCAGCTCAGGGT-3′) containing *Nco*I and *Eco*RI restriction sites, respectively. The PCR product, digested with *Nco*I and *Eco*RI endonucleases (Invitrogen), was cloned into the expression vector pPro-EX HTb (Invitrogen), which provides an N-terminal His_6 tag (H_6DYDIPTTENLYFQGAMG). The resulting construct, termed pPro-EX HTb^{miox}, was subsequently confirmed using DNA sequencing.

The pPro-EX HTb^{miox} construct was used to transform *Escherichia coli* BL21 (DE3) pRP cells (Novagen) for MIOX overexpression. The cells were grown in Luria–Bertani (LB) broth containing ampicillin (100 µg ml^{-1}) and chloramphenicol (34 µg ml^{-1}) at 310 K until the absorbance (OD_{600}) reached ∼0.9. The addition of 1 m*M* isopropyl *β*-D-thiogalactopyranoside (IPTG) initiated MIOX expression, which then proceeded for 12 h at 301 K. The cells were subsequently harvested by centrifugation for 15 min (3000*g*, 277 K) and resuspended in 50 m*M* Tris–HCl pH 8.0, 50 m*M* NaCl, 2 m*M* *β*-mercaptoethanol (buffer *A*) supplemented with EDTA-free protease-inhibitor tablets (Roche) and lysed using a cell disruptor (Constant Systems) at 124 MPa. To separate soluble and insoluble fractions, the lysis mixture was collected and centrifuged for 15 min (13 500*g*, 277 K). The supernatant, containing MIOX, was filtered through a 1.2 µm filter (Sartorius).

MIOX was purified using a three-step procedure. The first step, Ni^{2+}-affinity chromatography, utilized the N-terminal His_6 tag on MIOX. The lysate was applied onto a 5 ml Hi-Trap chelating column (Amersham Biosciences) charged with Ni^{2+}, followed by 10 ml buffer *A* containing 50 m*M* imidazole to remove non-specifically bound protein. To elute MIOX, buffer *A* containing 175 m*M* imidazole was applied until the absorbance (OD_{600}) returned to baseline. MIOX was incubated with recombinant tobacco etch virus (rTEV) protease for 12 h at 277 K to remove the His_6 tag, leaving four amino acids (GAMG) prior to the start methionine. The protein was then reapplied onto the Ni^{2+} column and eluted with buffer *A*, allowing further purification of MIOX from contaminants. Prior to a final purification step of size-exclusion chromatography, the protein solution was concentrated to a volume of 1 ml and incubated with 1 m*M* ammonium ferrous sulfate for 5 min. The enzyme was then applied onto an S200 HR10/30 column (Amersham Biosciences) pre-equilibrated in 50 m*M* MES pH 6.0, 50 m*M* NaCl, 2 m*M* TCEP (buffer *B*). MIOX eluted from the column as a single peak with a 16 ml retention volume. Based on both dynamic light-scattering results and the observed retention volume, it was concluded that MIOX is a monomeric protein (33 kDa), in agreement with previous studies (Arner *et al.*, 2006). The purified enzyme was incubated with 20 m*M* MI and concentrated to 20 mg ml^{-1} in buffer *B*. Absorbance readings (OD_{280}) of purified MIOX suggested a typical yield of 100 mg MIOX per litre of culture.

Circular-dichroism spectroscopy indicated that the purified enzyme was folded prior to crystallization. The recombinant protein did not display NADPH-binding characteristics as previously observed (Yang *et al.*, 2000). MIOX was shown to be active towards both MI and DCI in the presence of 1 m*M* Fe^{2+} and 2 m*M* L-cysteine using a colorimetric orcinol method for D-glucuronate detection (Reddy *et al.*, 1981). The protein was stored at 277 K for up to a week or 112 K indefinitely without precipitation or loss of activity.

2.2. Crystallization

The initial search for crystallization conditions was carried out with a Cartesian Honeybee dispensing system (Genomic Solutions), using a locally developed 480-condition crystallization screen (Moreland *et*

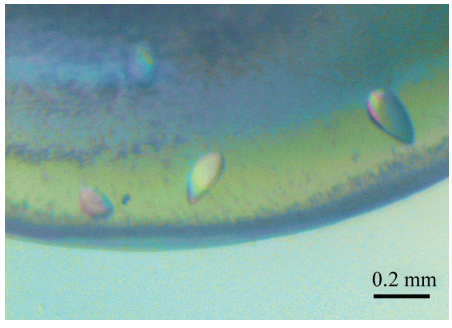

Figure 2
Crystals of MIOX grown from unbuffered 4.4 *M* sodium formate. Crystals appeared after one week and grew to approximately 0.1 × 0.2 × 0.05 mm after two weeks.

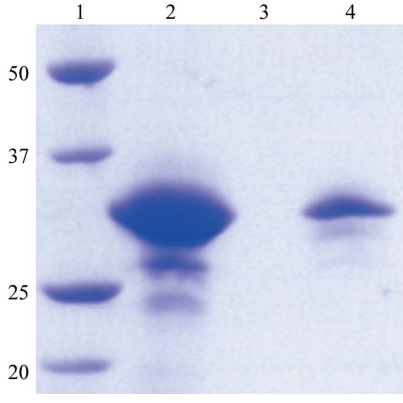

Figure 3
SDS–PAGE analysis of a dissolved crystal, highlighting the crystallization of the full-length enzyme. Lane 1, Precision Plus protein standards (kDa; BioRad); lane 2, semi-purified MIOX; lane 3, empty; lane 4, dissolved MIOX crystal (following extensive washing).

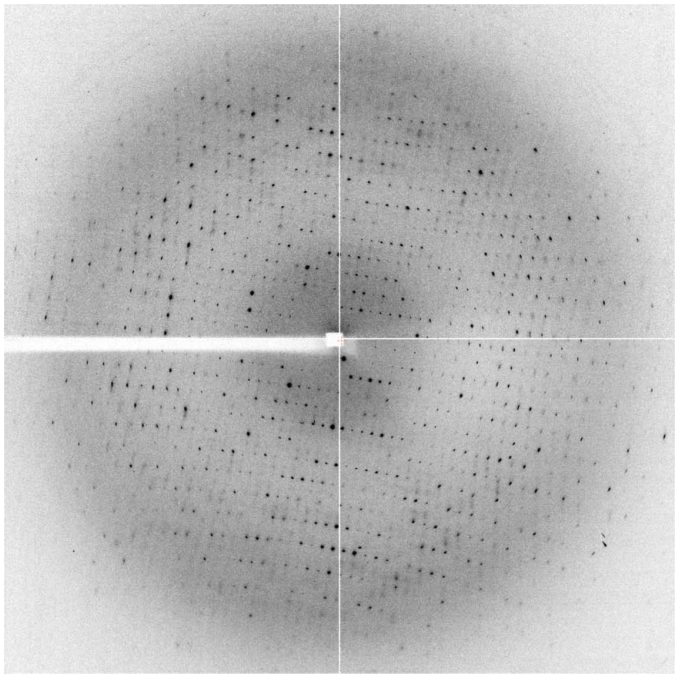

Figure 4
A 1.0° X-ray diffraction image from a native MIOX crystal. Crystals diffracted to 2.8 Å (edge of plate).

al., 2005) that included Hampton Research Crystal Screens I and II, Top 67, MPD, PEG/Ion and Precipitant Synergy screens. Experiments were performed using sitting-drop vapour diffusion at 291 K using 96-well Intelli-Plates (Hampton Research) containing 100 µl reservoir solution. Crystallization drops consisted of 100 nl protein solution (20 mg ml^{-1} in 50 m*M* MES pH 6.0, 50 m*M* NaCl, 2 m*M* TCEP, 20 m*M* MI) and 100 nl precipitant solution. Spherulites appeared in a condition comprising unbuffered 3.0 *M* sodium formate after one week.

VDX plates (Hampton) were used for fine screening around unbuffered 3.0 *M* sodium formate, producing crystals from unbuffered 4.4 *M* sodium formate (Fig. 2). The resulting mother liquor was shown to have a final pH of 6.5. Further variation of pH and the use of alternative salts or additives produced no improvement in the crystals, although increased drop sizes significantly enhanced crystal morphology.

Evidence from our laboratory and previous research (Arner *et al.*, 2006) shows that MIOX often degrades at the N-terminus to form a stable 30 kDa product. However, the MIOX crystals were analyzed by SDS–PAGE and were confirmed to be the full-length enzyme, as seen in Fig. 3.

2.3. Data collection and processing

Single MIOX crystals were transferred to a cryoprotectant solution consisting of 4.4 *M* sodium formate, 5% ethylene glycol for approximately 15 s before flash-cooling in liquid nitrogen. X-ray data were collected on beamline ID-29 at the European Synchrotron Radiation Facility (ESRF) using an ADSC Quantum-210 detector. Although most crystals diffracted anisotropically, crystal screening of diffraction patterns 90° apart allowed selection of a crystal with minimal anisotropic diffraction, resulting in a data set that was ∼97% complete to 2.8 Å resolution (Fig. 4).

The data were processed using *MOSFLM* (Leslie, 2006) and scaled with *SCALA* (Evans, 2006), giving the statistics shown in Table 1.

Table 1
Data-collection statistics.

Values in parentheses are for the outermost shell of data.

Wavelength (Å)	1.7389
Oscillation angle (°)	1.0
Resolution range (Å)	57.5–2.8 (2.95–2.80)
Unique reflections	7448 (1047)
Space group	$P2_12_12_1$
Unit-cell parameters (Å)	a = 44.87, b = 77.26, c = 84.84
Matthews coefficient (Å^3 Da^{-1})	2.2
Mosaicity (°)	0.8
Molecules per ASU	1
Solvent content (%)	44.4
Completeness (%)	97.1 (95.7)
Mean $I/\sigma(I)$	15.4 (3.7)
R_{sym}† (%)	0.060 (0.309)

† $R_{sym} = \sum_h \sum_i [|I_i(h) - \langle I(h)\rangle|] / \sum_h \sum_i I(h)]$, where I_i is the ith measurement and $\langle I(h)\rangle$ is the weighted mean of all measurements of $I(h)$.

As no homologous protein structures are currently available in the PDB, it is not possible to use molecular replacement for structure solution. In attempt to obtain phase information, selenomethionine substitution and heavy-metal incorporation experiments are under way. Furthermore, methods to improve crystal diffraction are being explored.

3. Summary

MIOX has received greater interest in recent years owing to the recognition of its importance in inositol regulation and diabetes aetiology. Crystallographic analysis of MIOX will provide a detailed description of the overall structure and active site of the enzyme, allowing a greater understanding of its novel mechanism. The preparation of diffraction-quality crystals of MIOX, reported here, represent an important first step towards this goal.

Special thanks are given to Dr Fasseli Coulibaly and Richard Bunker for help with data collection at ESRF. This research was supported by the Centre for Molecular Biodiscovery and Protemix. PB is a recipient of an Enterprise Scholarship from the Foundation for Research, Science and Technology.

References

Arner, R. J., Prabhu, K. S., Krishnan, V., Johnson, M. C. & Reddy, C. C. (2006). *Bichem. Biophys. Res. Commun.* **339**, 816–820.
Arner, R. J., Prabhu, K. S., Thompson, J. T., Hildenbrandt, G. R., Liken, A. D. & Reddy, C. C. (2001). *Biochem. J.* **360**, 313–320.
Brownlee, M. (2000). *Nature (London)*, **414**, 813–820.
Evans, P. (2006). *Acta Cryst.* D**62**, 72–82.
Khan, Z. A., Farhangkhoee, H., Mahon, J. L., Bere, L., Gonder, J. R., Chan, B. M., Uniyal, S. & Chakrabarti, S. (2006). *Exp Biol Med.* **231**, 1022–1029.
Leslie, A. G. W. (2006). *Acta Cryst.* D**62**, 48–57.
Moreland, N., Ashton, R., Baker, H. M., Ivanovic, I., Patterson, S., Arcus, V. L., Baker, E. N. & Lott, J. S. (2005). *Acta Cryst.* D**61**, 1378–1385.
Nayak, B., Xie, P., Akagi, S., Yang, G., Sun, L., Wada, J., Thakur, A., Danesh, F. R., Chugh, S. S. & Kanwar, Y. S. (2005). *Proc. Natl Acad. Sci. USA*, **102**, 17952–17957.
Ortmeyer, H. K., Huang, L. C., Zhang, L., Hansen, B. C. & Larner, J. (1993). *Endocrinology*, **132**, 646–651.
Reddy, C. C., Pierzchala, P. A. & Hamilton, G. A. (1981). *J. Biol. Chem.* **256**, 8519–8524.
Xing, G., Diao, Y., Hoffart, L. M., Barr, E. W., Prabhu, K. S., Arner, R. J., Reddy, C. C., Krebs, C. & Bollinger, J. M. (2006). *Proc. Natl Acad. Sci. USA*, **103**, 6130–6135.
Yang, Q., Dixit, B., Wada, J., Tian, Y., Wallner, E. I., Srivastva, S. K. & Kanwar, Y. S. (2000). *Proc. Natl Acad. Sci. USA*, **97**, 9896–9901.